



## Research Article

# Analysis of User Content Retrieval Delay Based on the Matern Hard-Core Point Process of Type II

Shuyuan Zhao <sup>1</sup>, Jihong Zhao,<sup>1,2</sup> Hua Qu,<sup>1,2</sup> and Gongye Ren <sup>1</sup>

<sup>1</sup>School of Electronic and Information Engineering, Xi'an Jiaotong University, Xi'an 710054, China

<sup>2</sup>School of Telecommunication and Information Engineering, Xi'an University of Posts and Telecommunications, Xi'an 710061, China

Correspondence should be addressed to Shuyuan Zhao; [dreamwonder@stu.xjtu.edu.cn](mailto:dreamwonder@stu.xjtu.edu.cn)

Received 14 June 2018; Revised 9 August 2018; Accepted 16 August 2018; Published 4 September 2018

Academic Editor: Alessandro Bazzi

Copyright © 2018 Shuyuan Zhao et al. This is an open access article distributed under the Creative Commons Attribution License, which permits unrestricted use, distribution, and reproduction in any medium, provided the original work is properly cited.

The content retrieval delay is an important performance metric for enhancing user experience in wireless networks. In this paper, by modeling the locations of the base stations (BSs) as the Matern hard-core point process of type II (MHP), we analyze the content retrieval delay for a typical cache-enabled device in wireless networks under the most popular content policy. Since it is intractable to get the size distribution of a Voronoi cell in the MHP model, we propose an approximate formula based on the empirical result in the Poisson point process and derive the cellular load which denotes the number of the user devices connected to a randomly chosen BS. Since the probability generating functional for MHP does not exist, we also propose approximate methods for the coverage probability of the MHP model. At last, we derive the cumulative distribution function of the content retrieval delay. Simulation results validate the accuracy of our analytical conclusions for user content retrieval delay.

## 1. Introduction

Over the past several years, the global mobile data traffic grows rapidly with the proliferation of smart terminals and is expected to increase to 30.6 exabytes per month by 2020 [1]. With the increasing demand for higher capacity and lower latency in wireless networks, the fifth generation (5G) wireless network has been proposed to improve the capacity of current networks by a factor of 1000 [2]. In recent years, studies show that a large portion of mobile data traffic is generated by repeated request of numerous popular contents [3]. Besides, the storage capacity of memory devices grows rapidly at a relatively low cost. Under these conditions, caching some popular contents at the network edge has been considered as a promising technique to alleviate the network traffic load and improve the quality of user service [4].

Key notions, challenges, and research topics of wireless caching were provided in [5]. Two methods of caching at the network edge have been studied in the literature: caching at helper nodes [6] and caching at the mobile devices (MDs) [7–9]. In this paper, we focus on the device caching solely and assume the contents are cached in the devices during off-peak

time (e.g., at night). Effective proactive caching policies can largely alleviate the burden of the base stations (BSs) during the peak hours, yielding high offloading gain [9–11].

The content retrieval delay is an important performance metric for enhancing user experience, and in order to give a detailed performance analysis, we consider a popular-based caching strategy called the most-popular-content (MPC) policy [12, 13] in this paper. The spatial distribution of BSs and mobile devices strongly affects the performance analysis of the wireless networks. In recent years, stochastic geometry has been utilized to model the wireless networks, and the Poisson point process (PPP) has been shown to be a tractable system model for its useful mathematical properties [14]. Most works [15–17] focus on the caching problems in a scenario where the BSs or the user devices are distributed according to a homogeneous PPP. However, the BSs in the PPP model are assumed to be distributed independently, which deviates from the fact that the locations of the BSs have strong correlation. Therefore, in this paper, we propose to use the Matern hard-core point process of type II (MHP) [18–21] to model the distribution of BSs, which is a more general and realistic model. Since the probability generating

functional (PGFL) for MHP does not exist, we focus on the approximation for the cellular load and coverage probability in carefully chosen cases.

The contributions of this paper are summarized as follows:

- (i) We analyze the content retrieval delay for a typical cache-enabled device with the MPC policy in the scenario where the BSs are distributed as the MHP model.
- (ii) We propose a reasonable approximation for the probability density function of the size of a typical Voronoi cell in the MHP model and confirm its effectiveness through the simulation of the cellular load.
- (iii) We evaluate the performance of two proposed methods for approximating the coverage probability in special cases and select the better one to calculate the delay.

The rest of this paper is organized as follows. In Section 2, we present our network and caching model and derive the cumulative distribution function of the content retrieval delay and then propose the approximation for the cellular load and coverage probability in the MHP model. In Section 3, we compare analytical results with the Monte Carlo simulation results. Finally, Section 4 provides our conclusions.

## 2. Analysis of User Content Retrieval Delay

**2.1. Network Model.** Consider a downlink cellular network consisting of BSs and MDs, and all BSs operate in full loaded state. We use MHP to model the actual spatial distribution of BSs. The MHP  $\Phi_m$  of BSs is generated from a PPP  $\Phi_p$  with density  $\lambda_p$  as follows: associate each point with a random mark  $m \sim U(0, 1)$ , and then delete a point if there exist other points within the distance  $d$  with a smaller mark. The density of  $\Phi_m$  is given by [19]

$$\lambda_m = \frac{(1 - \exp(-\lambda_p \pi d^2))}{\pi d^2}. \quad (1)$$

Besides, we assume the MDs in service are scattered randomly based on a stationary PPP  $\Phi_D$  with density  $\lambda_D$ , and each MD is connected to the nearest BS. So the cell area of each BS forms a Voronoi tessellation. Also, we consider the standard path loss propagation model with path loss exponent  $\alpha$  and assume that the small scale fading follows Rayleigh fading.

**2.2. Caching Model.** We assume that each MD requests only one file from a library of  $L$  files of equal size  $S$  bits at a time. The files are indexed according to their popularity, ranking from the most popular (the 1st file) to the least popular (the  $L_{th}$  file). The request probability of the  $i_{th}$  popular file follows the Zipf distribution [22]:

$$P_i = \frac{i^{-\sigma}}{\sum_{j=1}^L j^{-\sigma}}, \quad (2)$$

where  $\sigma$  characterizes the skewness of content popularity distribution.

According to the MPC policy, for simplicity, we assume that each MD has the same cache capacity and caches  $K$  ( $K \ll L$ ) most popular files, so the content hit probability denoted by  $P_{mpc}$  is

$$P_{mpc} = \frac{\sum_{i=1}^K i^{-\sigma}}{\sum_{j=1}^L j^{-\sigma}}. \quad (3)$$

So the user retrieval delay, denoted by  $T_d$ , happens when a content request is retrieved from the connected BS ( $T_d = 0$  means cache hit). Hence, the cumulative distribution function (CDF) of  $T_d$  can be calculated as

$$\begin{aligned} P(T_d < t) &= P\left(\frac{S}{R_d} < t\right) \\ &= (1 - P_{mpc})P\left(R_d > \frac{S}{t}\right) + P_{mpc}. \end{aligned} \quad (4)$$

Considering the effect of the TDMA scheduling, the data rate  $R_d$  is given by [23]

$$R_d = \frac{B}{N} \log(1 + SINR_d), \quad (5)$$

where  $N$  denotes the cellular load which means the total number of MDs served by the associated BS at the same time. With the assumption that all BSs operate in full loaded state, the complementary cumulative distribution function (CCDF) of  $R_d$  can be derived by the distribution of  $N$  and  $SINR_d$  as follows:

$$\begin{aligned} P\left(R_d > \frac{S}{t}\right) &= P\left(SINR_d > 2^{\frac{SN}{tB}} - 1\right) \\ &= \sum_{n=1}^{\infty} P(N = n | N \geq 1) \\ &\quad \cdot P\left(SINR_d > 2^{\frac{SN}{tB}} - 1 | N = n\right), \end{aligned} \quad (6)$$

where  $P(N = n)$  denotes the probability mass function of the cellular load  $N$  and  $P(SINR_d > 2^{\frac{SN}{tB}} - 1)$  denotes the coverage probability of the MHP model. They will be derived in the following sections.

**2.3. Probability of the Cellular Load.** The probability mass function of the cellular load  $N$  in a typical Voronoi cell can be given by the law of total probability as follows:

$$P(N = n) = \int_0^{\infty} P(N = n | X = x) \cdot f_X(x) dx, \quad (7)$$

where  $X$  denotes the size of a typical Voronoi cell and  $f_X(x)$  denotes the probability density function of it. However, we cannot determine  $f_X(x)$  in the MHP model directly, a problem that has not been studied in the literature before. So firstly we consider the situation that the BSs are distributed as a homogeneous PPP  $\Phi_p$  with density  $\lambda_p$ . The normalized size

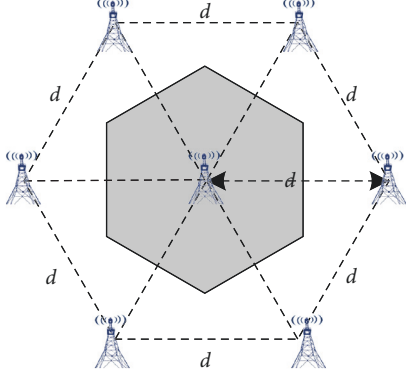


FIGURE 1: The minimum size of a typical Voronoi cell in the MHP model with a minimum distance  $d$ .

distribution function of Poisson Voronoi cells is accurately approximated in [24] by the Monte Carlo method:

$$f_p(x) = \frac{3.5^{3.5}}{\Gamma(3.5)} x^{2.5} e^{-3.5x}, \quad (8)$$

where  $x$  denotes the random variable of a cell size normalized by the value  $1/\lambda_p$ .

Consider an MHP  $\Phi_m$  of density  $\lambda_m$  with a minimum distance  $d$  generated from the PPP  $\Phi_p$  with density  $\lambda_p$  as mentioned above. We can get the minimum cell size in the situation that the distance between the target BS and all neighbor BSs is  $d$ , as shown in Figure 1:  $S_{\min} = \sqrt{3}d^2/2$ . When  $d$  is small enough, there are very few cases that the distance between two BSs is less than  $d$ . So ignoring the invalid situations  $x < S_{\min}$ ,  $f_m(x)$  is close to  $f_p(x)$  when  $d$  is small

enough. Compared with  $f_p(x)$ , we can give an approximation for the normalized size distribution of a Voronoi cell of the MHP model, denoted by  $f_m(x)$ :

$$f_m(x) \approx \begin{cases} 0, & x \in [0, S_{\min}) \\ \frac{f_p(x)}{\left(1 - \int_0^{S_{\min}\lambda_m} f_p(x) dx\right)}, & x \in [S_{\min}, +\infty). \end{cases} \quad (9)$$

Notice that  $x$  is normalized by the value  $1/\lambda_m$ . When  $x \in [S_{\min}, +\infty)$ ,  $f_m(x)$  can be simplified as follows:

$$\begin{aligned} f_m(x) &\approx \frac{f_p(x)}{\left(1 - \int_0^{S_{\min}\lambda_m} f_p(x) dx\right)} \\ &= \frac{3.5^{3.5} x^{2.5} e^{-3.5x} / \Gamma(3.5)}{1 - \int_0^{S_{\min}\lambda_m} 3.5^{3.5} x^{2.5} e^{-3.5x} / \Gamma(3.5) dx} \\ &\stackrel{(a)}{=} \frac{3.5^{3.5} \cdot x^{2.5} e^{-3.5x}}{\Gamma(3.5) - \gamma(3.5, 7S_{\min}\lambda_m/2)}, \end{aligned} \quad (10)$$

where (a) follows:  $\int_0^u x^{v-1} e^{-\mu x} dx = \mu^{-v} \gamma(v, \mu u)$  [25], and  $\gamma(v, t) = \int_0^t x^{v-1} e^{-x} dx$  denotes the lower incomplete gamma function. So the probability mass function of the cellular load in the MHP model can be derived in the following theorem, according to (7) and (10).

**Theorem 1.** *When  $d$  is small enough, the probability mass function of the cellular load in the MHP model can be approximated by*

$$P(N = n) = \frac{3.5^{3.5} (\lambda_D/\lambda_m)^n (\lambda_D/\lambda_m + 3.5)^{-(n+3.5)} \Gamma(n + 3.5, S_{\min} (\lambda_D/\lambda_m + 3.5) \lambda_m)}{(\Gamma(3.5) - \gamma(3.5, 7S_{\min}\lambda_m/2)) n!}, \quad (11)$$

and

$$P(N = n | N \geq 1) = \frac{P(N = n)}{(1 - P(N = 0))}. \quad (12)$$

*Proof.* See Appendix A.  $\square$

Considering general cases, when  $d$  is a random variable, compared  $f_m(x)$  with  $f_p(x)$  which have the same density  $\lambda$ , we can find several useful characteristics of  $f_m(x)$  as follows obviously:

- (1) When  $x \rightarrow S_{\min}$ ,  $f_m(x) \rightarrow 0$ .
- (2) When  $d \rightarrow 0$ ,  $f_m(x) \rightarrow f_p(x)$ .
- (3) For a specific value of  $x$ ,

$f_p(x) = x\{\text{no BS closer than } d\} + x\{\text{at least one BS closer than } d\}$ /all situations and  $f_m(x) = x\{\text{no BS closer than } d\}$ /all situations  $\setminus$   $x\{\text{no BS closer than } d\}$ , where  $x\{\text{no BS}$

*closer than } d\} denotes the situations that a cell has a size of  $x$  and there is no BS located closer than  $d$ , and  $x\{\text{at least one BS closer than } d\}$  denotes the situations that a cell has a size of  $x$  and there is at least one BS located closer than  $d$ . For all  $x$ , the situations  $x\{\text{at least one BS closer than } d\}$  can be considered as a relatively fixed value, so we can get that  $f_m(x)/f_p(x)$  increases with the increase of  $f_p(x)$ .*

Based on the three characteristics mentioned above, we consider a conjecture of  $f_m(x)$  as follows:

$$f_m(x) = C \times \left( \frac{3.5^{3.5}}{\Gamma(3.5)} x^{2.5} e^{-3.5x} \right)^{1+\gamma} \times \frac{x - S}{x}, \quad (13)$$

where  $C$  denotes the bias and  $\gamma$  denotes a predefined constant depending on the value of  $\lambda_m$  and  $d$ . Since  $\int_{S_{\min}}^{\infty} f_m(x) dx = 1$ , we can get

C

$$= \frac{\Gamma(3.5)^{1+\gamma}}{3.5^{3.5(1+\gamma)} \times \left[ (3.5 + 3.5\gamma)^{-(3.5+2.5\gamma)} \Gamma(3.5 + 2.5\gamma, 3.5S_{\min}(1+\gamma)) - S_{\min}(3.5 + 3.5\gamma)^{-(2.5+2.5\gamma)} \Gamma(2.5 + 2.5\gamma, 3.5S_{\min}(1+\gamma)) \right]} \quad (14)$$

Similar to (11), the probability mass function of the cellular load in the MHP model can be derived in the following theorem.

**Theorem 2.** *When  $d$  is a random variable, the probability mass function of the cellular load in the MHP model is*

$$\begin{aligned} P(N = n) &= C \frac{3.5^{3.5(1+\gamma)} (\lambda_D/\lambda_m)^n}{\Gamma(3.5)^{1+\gamma} n!} \\ &\times \left[ \left( \frac{\lambda_D}{\lambda_m} + 3.5(1+\gamma) \right)^{-(n+3.5+2.5\gamma)} \right. \\ &\cdot \Gamma\left( n + 3.5 + 2.5\gamma, \left( \frac{\lambda_D}{\lambda_m} + 3.5(1+\gamma) \right) S_{\min} \right) \\ &- S_{\min} \left( \frac{\lambda_D}{\lambda_m} + 3.5(1+\gamma) \right)^{-(n+2.5+2.5\gamma)} \\ &\left. \cdot \Gamma\left( n + 2.5 + 2.5\gamma, \left( \frac{\lambda_D}{\lambda_m} + 3.5(1+\gamma) \right) S_{\min} \right) \right], \quad (15) \end{aligned}$$

where  $\gamma$  is a predefined constant depending on the value of  $\lambda_m$  and  $d$ .

*Proof.* See Appendix B.  $\square$

In Section 3, we give detailed numerical simulation about the conjecture and can get that if  $\gamma$  is appropriately predefined, the analysis (15) suits the simulation result well.

**2.4. Approximation of the Coverage Probability.** The proposed interference model is illustrated in Figure 2. Since MHP is a stationary point process, we assume that the attached BS

is located at the origin without loss of generality.  $r$  denotes the distance between MD and the attached BS,  $v$  denotes the distance between the attached BS and any interfering BS, and  $l_i$  denotes the distance between MD and any interfering BS  $i$ ,  $l_i = \sqrt{v^2 + r^2 - 2rv \cos(\theta - \varphi)}$ . We assume that the small scale fading follows Rayleigh fading,  $h \sim \exp(\mu)$ , and the noise is neglected,  $\sigma^2 = 0$ . The MD is in coverage when its  $SINR_d$  is larger than some threshold  $T$ . So we can get the following lemma.

**Lemma 3.** *The coverage probability of a typical MD can be given by*

$$\begin{aligned} P(SINR_d > T) \\ = \int_0^{2\pi} \int_0^\infty \frac{f(r)}{2\pi} \mathbb{E}_{\Phi_m}^{\text{lo}} \left( \prod_{i \in \Phi_m} \frac{1}{1 + Tr^\alpha l_i^{-\alpha}} \right) dr d\varphi, \quad (16) \end{aligned}$$

where  $f(r)$  is the probability density function of the distance between a typical MD and its associated BS, which can be approximated as follows [26]:

$$f(r) = 2\pi\lambda_m r e^{-\pi\lambda_m r^2}. \quad (17)$$

*Proof.* See Appendix C.  $\square$

Since the PGFL of MHP is unknown, it is difficult to get the exact value of  $\mathbb{E}_{\Phi_m}^{\text{lo}} \left( \prod_{i \in \Phi_m} (1/(1 + Tr^\alpha l_i^{-\alpha})) \right)$ . So in this paper, we consider several reasonable approximations for the coverage probability of the MHP model in different situations. We first give the second-order product density  $\rho_m^2(v)$  of the MHP [19] which will be used in the following approximations:

$$\rho_m^2(v) = \begin{cases} \lambda_m^2, & \text{if } v \geq 2d \\ \frac{2V(v) [1 - \exp(-\lambda_p \pi d^2)] - 2\pi d^2 [1 - \exp(-\lambda_p V(v))]}{\pi d^2 V(v) [V(v) - \pi d^2]}, & \text{if } 2d > v \geq d \\ 0, & \text{if } v < d, \end{cases} \quad (18)$$

$$V(v) = 2\pi d^2 - 2d^2 \cos^{-1} \left( \frac{v}{2d} \right) + v \sqrt{d^2 - \frac{v^2}{4}}. \quad (19)$$

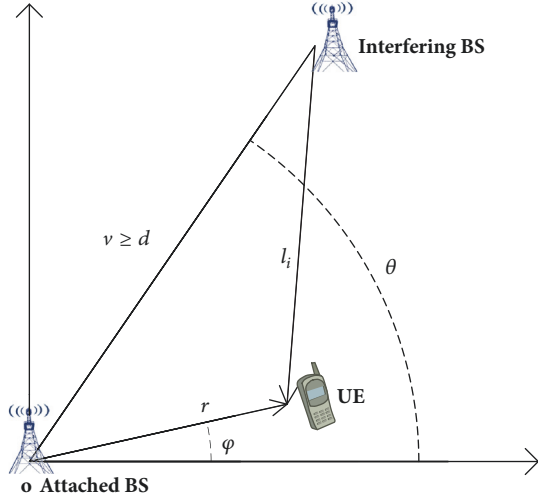


FIGURE 2: The interference model, where the attached BS is located at the origin.

Then we analyze the coverage probability as follows:

(1) Considering general cases, when  $d$  is a random non-negative variable, we consider two methods to approximate the coverage probability, as shown in the following two propositions.

**Proposition 4.** A rough approximation for the coverage probability of a typical MD using the second-order Taylor expansion can be given by

$$P_1 (SINR_d > T) \approx \int_0^{2\pi} \int_0^{\infty} \lambda_m r e^{-\pi \lambda_m r^2} \omega dr d\varphi, \quad (20)$$

where

$$\begin{aligned} \omega &\approx 1 - \lambda_m^{-1} \int_{\mathbb{R}^2} \rho_m^2(v) g_1(r, v, \theta, \varphi) dx + \frac{1}{2} \\ &\cdot \lambda_m^{-1} \int_{\mathbb{R}^2} \rho_m^2(v) g_1^2(r, v, \theta, \varphi) dx = 1 \\ &- \lambda_m^{-1} \int_0^{2\pi} \int_0^{\infty} \int_{\max[d, |2r \cos(\theta - \varphi)|]}^{\infty} \rho_m^2(v) g_1(r, v, \theta, \varphi) \\ &\cdot v dv d\theta + \frac{1}{2} \lambda_m^{-1} \int_0^{2\pi} \int_0^{\infty} \int_{\max[d, |2r \cos(\theta - \varphi)|]}^{\infty} \rho_m^2(v) \\ &\cdot g_1^2(r, v, \theta, \varphi) v dv d\theta, \\ g_1(r, v, \theta, \varphi) &= \ln \left( 1 \right. \\ &\left. + T \left( \frac{r^2}{v^2 + r^2 - 2rv \cos(\theta - \varphi)} \right)^{\alpha/2} \right). \end{aligned} \quad (22)$$

*Proof.* See Appendix D.  $\square$

**Proposition 5.** A lower bound for the coverage probability using Jensen's inequality is given by

$$P_1 (SINR_d > T) \geq \int_0^{2\pi} \int_0^{\infty} \lambda_m r e^{-\pi \lambda_m r^2} e^{-\eta} dr d\varphi, \quad (23)$$

where

$$\begin{aligned} \eta &= \lambda_m^{-1} \int_0^{2\pi} \int_0^{\infty} \int_{\max[d, |2r \cos(\theta - \varphi)|]}^{\infty} \rho_m^2(v) g_1(r, v, \theta, \varphi) \\ &\cdot v dv d\theta. \end{aligned} \quad (24)$$

*Proof.* See Appendix E.  $\square$

(2) When  $d$  is small enough, according to Proposition 1 in [26], a lower bound is given by

$$P_2 (SINR_d > T) \geq \int_0^{2\pi} \int_0^{\infty} \lambda_m r e^{-\pi \lambda_m r^2} e^{-\zeta} dr d\varphi, \quad (25)$$

where

$$\begin{aligned} \zeta &= \lambda_m^{-1} \int_0^{2\pi} \int_0^{\infty} \int_{\max[d, |2r \cos(\theta - \varphi)|]}^{\infty} \rho_m^2(v) g_2(r, v, \theta, \varphi) \\ &\cdot v dv d\theta, \end{aligned} \quad (26)$$

$$\begin{aligned} g_2(r, v, \theta, \varphi) &= \left[ 1 \right. \\ &\left. + T^{-1} \left( \frac{r^2}{v^2 + r^2 - 2rv \cos(\theta - \varphi)} \right)^{-\alpha/2} \right]^{-1}. \end{aligned} \quad (27)$$

According to the analysis proposed above, we will evaluate the performance of the approximations for the cellular load and coverage probability with numerical results in different situations, mainly including Theorems 1, 2, Propositions 4, 5, and lower bound (25). Also, the content retrieval delay will be simulated according to (4) and (6).

### 3. Numerical Results

In this section, we evaluate the performance of the proposed approximations for the cellular load and the coverage probability both in general cases and in special cases ( $d$  is small enough) and validate the accuracy of the numerical results for user content retrieval delay with the MPC policy.

**3.1. Simulation Setup.** The simulation is conducted in a square area with side length 3km. The MHP model of BSs is generated from a PPP model with the density  $\lambda_p = 5 \times 10^{-6}/\text{m}^2$ . The density of MDs is  $\lambda_D = 5 \times 10^{-5}/\text{m}^2$ . The

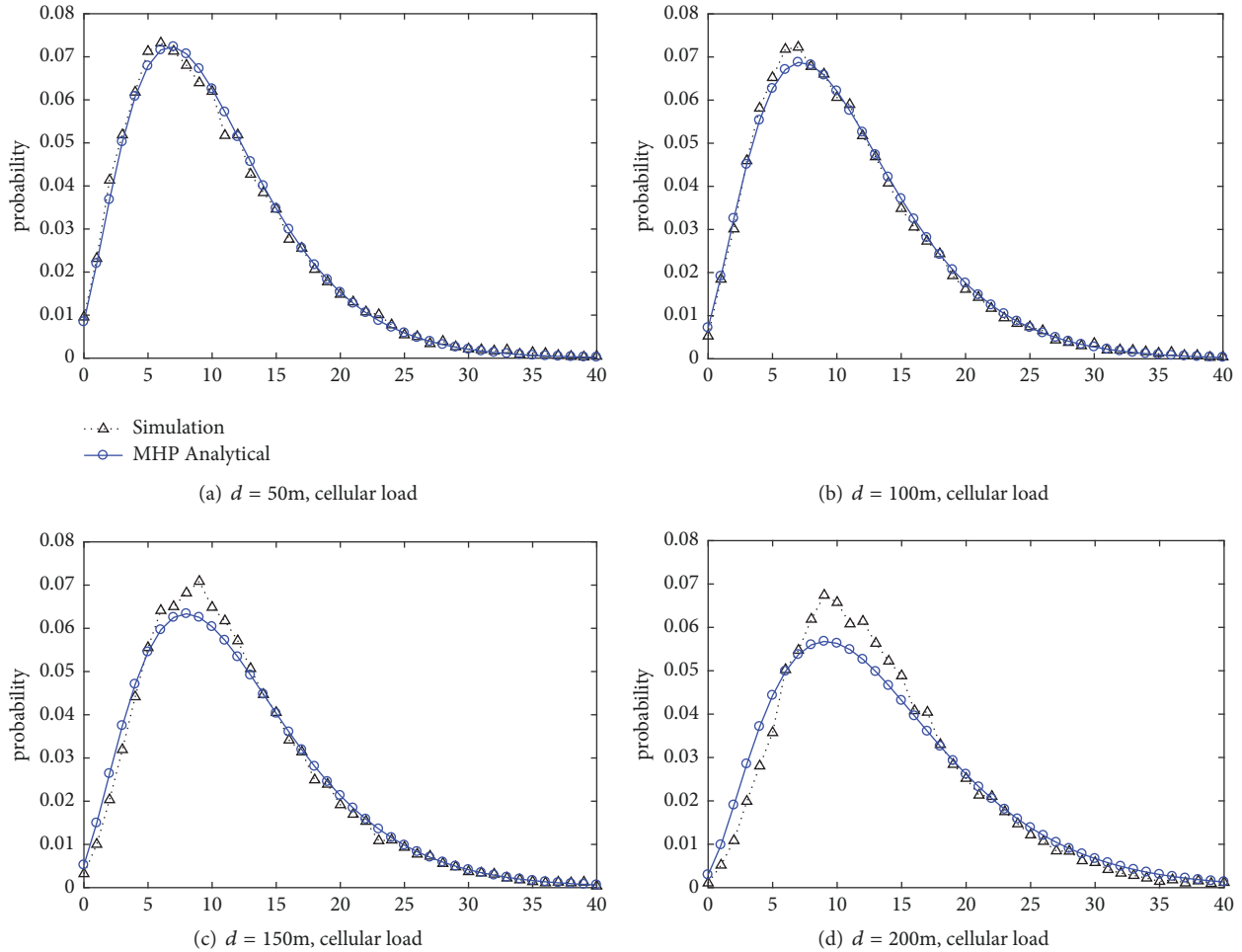


FIGURE 3: Numerical results of the cellular load with (11), compared with the simulation results. (a)  $d = 50\text{m}$ , (b)  $d = 100\text{m}$ , (c)  $d = 150\text{m}$ , and (d)  $d = 200\text{m}$ .

bandwidth of all BSs is 20 MHz, and the path loss parameter is 4. The size of the file library is 1000, and the size of each file is 100 Mbits. In the MPC policy, each MD can cache 50 files.

**3.2. The Cellular Load Simulation.** According to (10) and (11), we get the analytical results of the cellular load in the MHP model as shown in Figure 3. It is impressive that the numerical results closely match the simulation results when  $d$  is small enough as shown in Figures 3(a) and 3(b), and it also means that the approximate size distribution of the MHP model is effective. But in general cases, when  $d$  is 150, 200m or larger, it seems that the approximation of (10) does not work well as shown in Figures 3(c) and 3(d).

In Figure 4, we conduct the simulation of the conjecture for the size distribution and cellular load in general cases according to (13) and (15). We can easily find that  $\gamma$  has notable positive correlation with  $d$  and when  $d = 200, 300, 400\text{m}$ , the numerical results agree well with the simulation results with the parameter  $\gamma = 0.4, 0.8, 1.2$ , respectively. This is because with the increase of  $d$ , the situations  $x\{\text{at least one BS closer than } d\}$  become greater,

which leads to the greater change of  $f_m(x)/f_p(x)$ , and the value of  $\gamma$  should be predefined larger then. By comparing the numerical with simulation results, the conjecture (13) proposed above will work well when  $\gamma$  is carefully predefined according to  $d$ .

**3.3. The Coverage Probability Simulation.** In Figure 5, we evaluate the performance of Propositions 4 and 5 and lower bound (25) with the MHP model of  $d = 50\text{m}$  and  $d = 300\text{m}$ , respectively. Although the lower bound (25) is not very close to the simulation results when  $d = 300\text{m}$ , it still performs much better than (20) and (23). Therefore, we will always use the lower bound (25) for the coverage probability to conduct the simulation of the user content retrieval delay.

**3.4. User Content Retrieval Delay Simulation.** In Figure 6, we use Theorem 1 and (25) together to analyze the content retrieval delay when  $d = 50\text{m}$ , while Theorem 2 and (25) are used when  $d = 300\text{m}$ . Figure 6 shows that the analytical results are close to the simulation results, and the CDF of the content retrieval delay increases with the growth of the

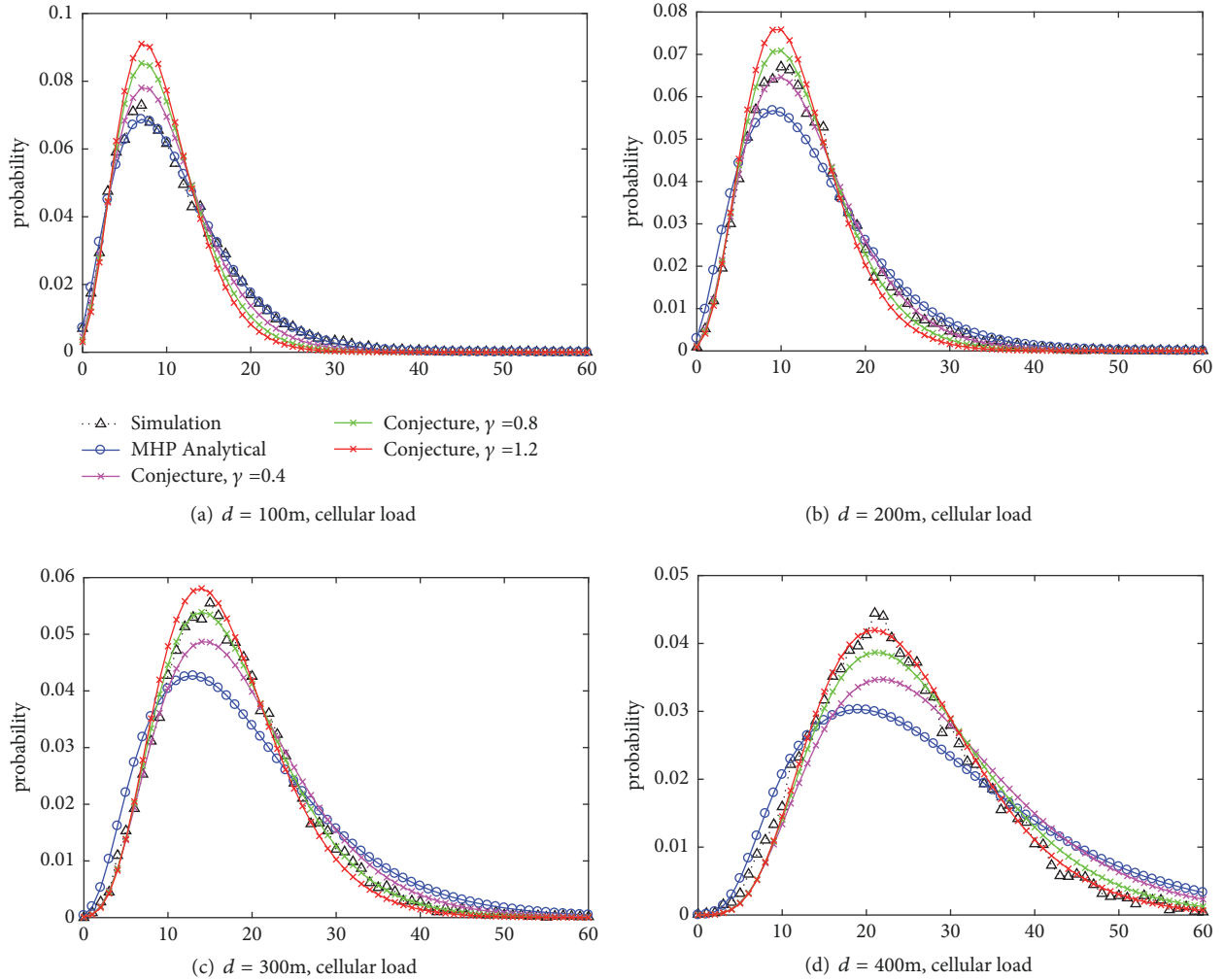


FIGURE 4: Numerical results of the cellular load with conjecture (15),  $\gamma = 0.4, 0.8, 1.2$ , compared with (11) and the simulation results. (a)  $d = 100\text{m}$ , (b)  $d = 200\text{m}$ , (c)  $d = 300\text{m}$ , and (d)  $d = 400\text{m}$ .

popularity exponent  $\sigma$ , since MDs can get the requested content from themselves more probably.

According to the numerical results above, we can get the following conclusions:

- (1) When  $d$  is small enough, Theorem 1 for the cellular load and lower bound (25) for the coverage probability performs well compared with the simulation results.
- (2) When  $d$  is a random nonnegative variable, especially when  $d$  is large, Theorem 2 for the cellular load with carefully predefined  $\gamma$  performs well. Besides, although lower bound (25) is derived when  $d$  is small enough, it still performs better than Propositions 4 and 5.

## 4. Conclusions

We analyze the content retrieval delay of cache-enabled devices in wireless networks, by modeling the distribution

of the BSs with the MHP. Due to the intractability of the MHP, we give some approximations of the cellular load and the coverage probability, both in general cases and in special cases for numerical evaluation. The simulations show that our approximations are reasonable and accurate. The approximations of the MHP are quite useful for the analysis in the cache-enabled networks, and we only consider the simplest scenario with the baseline caching strategy to verify the reliability in this paper. As a promising future direction, we will focus on the optimization of the probabilistic caching strategy for maximizing the cache hit probability or the successful delivery probability of the requested content.

## Appendix

### A. Proof of Theorem 1

According to (7) and (10), we can get

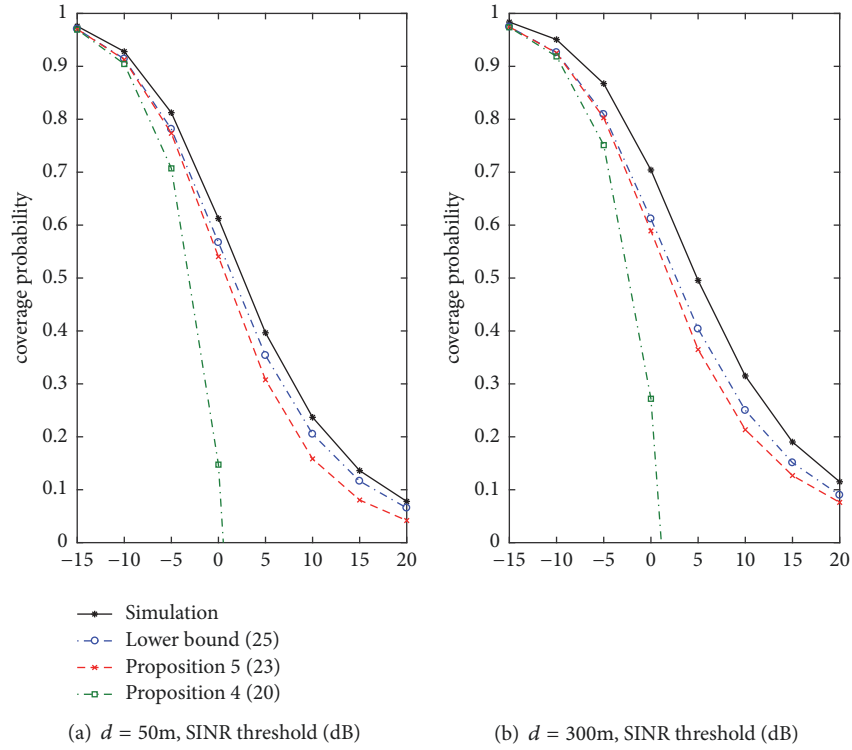


FIGURE 5: Coverage probability based on Propositions 4 and 5 and lower bound (25), compared with the simulation results,  $d = 50\text{m}$  and  $d = 300\text{m}$ .

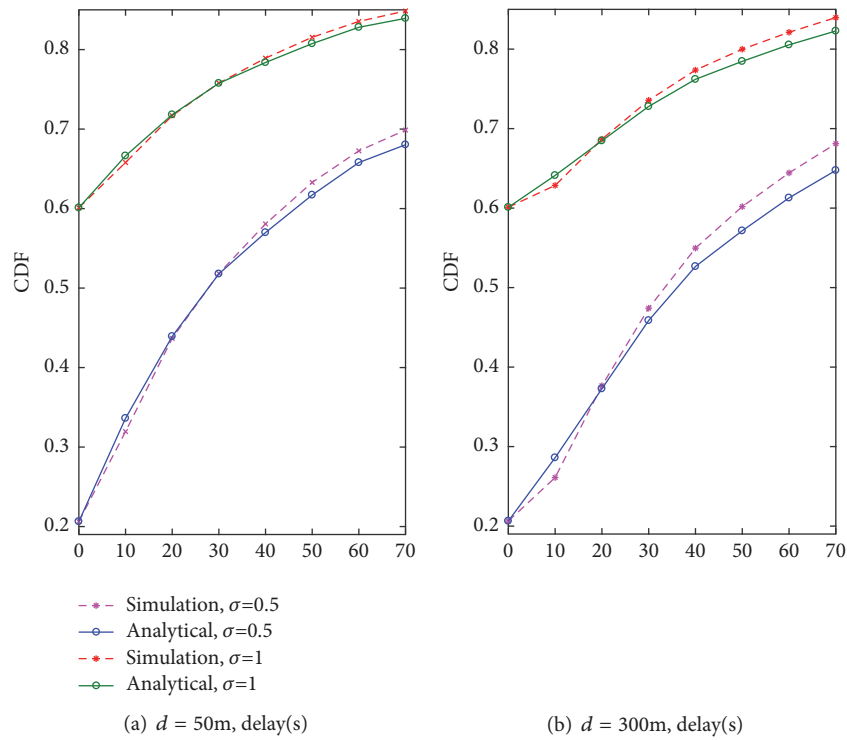


FIGURE 6: CDF of the user content retrieval delay,  $d = 50\text{m}$  and  $d = 300\text{m}$ .



$$\begin{aligned}
P(N = n) &= \int_0^\infty P(N = n | x) \cdot f_m(x) dx = \int_0^\infty \frac{(\lambda_D(x/\lambda_m))^n}{n!} e^{-\lambda_D(x/\lambda_m)} \cdot f_m(x) dx \\
&\approx \frac{3.5^{3.5} (\lambda_D/\lambda_m)^n}{(\Gamma(3.5) - \gamma(3.5, 7S_{\min}\lambda_m/2)) n!} \times \int_{S_{\min}\lambda_m}^\infty x^{n+2.5} e^{-(\lambda_D/\lambda_m+3.5)x} dx \\
&\stackrel{(a)}{=} \frac{3.5^{3.5} (\lambda_D/\lambda_m)^n (\lambda_D/\lambda_m + 3.5)^{-(n+3.5)} \Gamma(n+3.5, S_{\min}(\lambda_D/\lambda_m + 3.5)\lambda_m)}{(\Gamma(3.5) - \gamma(3.5, 7S_{\min}\lambda_m/2)) n!},
\end{aligned} \tag{A.1}$$

where (a) follows  $\int_u^\infty x^{v-1} e^{-\mu x} dx = \mu^{-v} \Gamma(v, \mu u)$  [25] and  $\int_0^u x^{v-1} e^{-\mu x} dx = \mu^{-v} \gamma(v, \mu u)$ .  $\Gamma(v, t) = \int_t^\infty x^{v-1} e^{-x} dx$  denotes the upper incomplete gamma function. In Section 3, the simulation results confirm the effectiveness of the approximation when  $d$  is small enough.

## B. Proof of Theorem 2

According to (7), (13), and (14), when  $d$  is a random variable, the probability mass function can be given by

$$\begin{aligned}
P(N = n) &= \int_0^\infty P(N = n | x) \cdot f_m(x) dx \\
&= \int_0^\infty \frac{(\lambda_D(x/\lambda_m))^n}{n!} e^{-\lambda_D(x/\lambda_m)} \left[ C \left( \frac{3.5^{3.5}}{\Gamma(3.5)} x^{2.5} e^{-3.5x} \right)^{1+\gamma} \right. \\
&\quad \cdot \left. \frac{x - S_{\min}}{x} \right] dx = C \\
&\quad \cdot \frac{3.5^{3.5(1+\gamma)} (\lambda_D/\lambda_m)^n}{\Gamma(3.5)^{1+\gamma} n!} \left[ \int_{S_{\min}}^\infty x^{n+2.5(1+\gamma)} e^{-(\lambda_D/\lambda_m+3.5(1+\gamma))x} dx \right. \\
&\quad \left. - S_{\min} \int_{S_{\min}}^\infty x^{n+1.5+2.5\gamma} e^{-(\lambda_D/\lambda_m+3.5(1+\gamma))x} dx \right] = C \\
&\quad \cdot \frac{3.5^{3.5(1+\gamma)} (\lambda_D/\lambda_m)^n}{\Gamma(3.5)^{1+\gamma} n!} \times \left[ \left( \frac{\lambda_D}{\lambda_m} + 3.5(1+\gamma) \right)^{-(n+3.5+2.5\gamma)} \right. \\
&\quad \cdot \Gamma(n+3.5+2.5\gamma, \left( \frac{\lambda_D}{\lambda_m} + 3.5(1+\gamma) \right) S_{\min}) \\
&\quad \left. - S_{\min} \left( \frac{\lambda_D}{\lambda_m} + 3.5(1+\gamma) \right)^{-(n+2.5+2.5\gamma)} \right. \\
&\quad \left. \cdot \Gamma(n+2.5+2.5\gamma, \left( \frac{\lambda_D}{\lambda_m} + 3.5(1+\gamma) \right) S_{\min}) \right],
\end{aligned} \tag{B.1}$$

where the last step follows:  $\int_u^\infty x^{v-1} e^{-\mu x} dx = \mu^{-v} \Gamma(v, \mu u)$  [25].

## C. Proof of Lemma 3

$$\begin{aligned}
P(\text{SINR}_d > T) &= \mathbb{E}_{r, \varphi} [\mathbb{P}(\text{SINR}_d > T | r, \varphi)] \\
&= \mathbb{E}_{r, \varphi} \left[ \mathbb{P} \left( \frac{hr^{-\alpha}}{\sigma^2 + I} > T | r, \varphi \right) \right] = \int_0^{2\pi} \int_0^\infty \frac{f(r)}{2\pi}
\end{aligned}$$

$$\begin{aligned}
&\cdot \mathbb{P}(h > T(\sigma^2 + I)r^\alpha | r, \varphi) dr d\varphi \\
&\stackrel{(a)}{=} \int_0^{2\pi} \int_0^\infty \frac{f(r)}{2\pi} \\
&\quad \cdot \mathbb{E}_{\Phi_m, I_i}^{\text{lo}} \left[ \exp \left( -T\mu r^\alpha \sum_{i \in \Phi_m} g_i l_i^{-\alpha} \right) \right] dr d\varphi \\
&= \int_0^{2\pi} \int_0^\infty \frac{f(r)}{2\pi} \\
&\quad \cdot \mathbb{E}_{\Phi_m}^{\text{lo}} \left[ \prod_{i \in \Phi_m} \mathbb{E}_{g_i} (\exp(-T\mu r^\alpha g_i l_i^{-\alpha})) \right] dr d\varphi \\
&\stackrel{(b)}{=} \int_0^{2\pi} \int_0^\infty \frac{f(r)}{2\pi} \\
&\quad \cdot \mathbb{E}_{\Phi_m}^{\text{lo}} \left( \prod_{i \in \Phi_m} \frac{1}{1 + T\mu r^\alpha l_i^{-\alpha}} \right) dr d\varphi,
\end{aligned} \tag{C.1}$$

where (a) and (b) follows:  $h, g_i \sim \exp(\mu)$ .

## D. Proof of Proposition 4

We consider using the second-order Taylor expansion to approximate  $\mathbb{E}_{\Phi_m}^{\text{lo}} (\prod_{i \in \Phi_m} (1/(1 + T\mu r^\alpha l_i^{-\alpha})))$  as follows:

$$\begin{aligned}
&\mathbb{E}_{\Phi_m}^{\text{lo}} \left( \prod_{i \in \Phi_m} \frac{1}{1 + T\mu r^\alpha l_i^{-\alpha}} \right) \\
&= \mathbb{E}_{\Phi_m}^{\text{lo}} \left[ \exp \left( - \sum_{i \in \Phi_m} \ln(1 + T\mu r^\alpha l_i^{-\alpha}) \right) \right] \\
&\approx \mathbb{E}_{\Phi_m}^{\text{lo}} \left[ 1 + \left( - \sum_{i \in \Phi_m} \ln(1 + T\mu r^\alpha l_i^{-\alpha}) \right) \right. \\
&\quad \left. + \frac{1}{2} \left( - \sum_{i \in \Phi_m} \ln(1 + T\mu r^\alpha l_i^{-\alpha}) \right)^2 \right] = 1
\end{aligned}$$

$$\begin{aligned}
& + \mathbb{E}_{\Phi_m}^{\text{lo}} \left( - \sum_{i \in \Phi_m} \ln(1 + Tr^\alpha l_i^{-\alpha}) \right) + \frac{1}{2} \\
& \cdot \mathbb{E}_{\Phi_m}^{\text{lo}} \left( - \sum_{i \in \Phi_m} \ln(1 + Tr^\alpha l_i^{-\alpha}) \right)^2 \geq 1 \\
& + \mathbb{E}_{\Phi_m}^{\text{lo}} \left( - \sum_{i \in \Phi_m} \ln(1 + Tr^\alpha l_i^{-\alpha}) \right) + \frac{1}{2} \\
& \cdot \mathbb{E}_{\Phi_m}^{\text{lo}} \left( \sum_{i \in \Phi_m} (\ln(1 + Tr^\alpha l_i^{-\alpha}))^2 \right). \tag{D.1}
\end{aligned}$$

Using (19) in [27], we can get that

$$\mathbb{E}_{\Phi_m}^{\text{lo}} \left[ \sum_{x \in \Phi_m} g(x) \right] = \lambda^{-1} \int_{\mathbb{R}^2} \rho_m^2(x) g(x) dx. \tag{D.2}$$

Let  $g_1(i) = g_1(r, v, \theta, \varphi) = \ln(1 + Tr^\alpha l_i^{-\alpha})$ ,  $\omega = \mathbb{E}_{\Phi_m}^{\text{lo}} (\prod_{i \in \Phi_m} (1/(1 + Tr^\alpha l_i^{-\alpha})))$ ; we can get

$$\begin{aligned}
\omega & \approx 1 - \lambda_m^{-1} \int_{\mathbb{R}^2} \rho_m^2(v) g_1(r, v, \theta, \varphi) dx + \frac{1}{2} \\
& \cdot \lambda_m^{-1} \int_{\mathbb{R}^2} \rho_m^2(v) g_1^2(r, v, \theta, \varphi) dx = 1 \\
& - \lambda_m^{-1} \int_0^{2\pi} \int_{\max[d, |2r \cos(\theta - \varphi)]}^{\infty} \rho_m^2(v) g_1(r, v, \theta, \varphi) \\
& \cdot v dv d\theta + \frac{1}{2} \lambda_m^{-1} \int_0^{2\pi} \int_{\max[d, |2r \cos(\theta - \varphi)]}^{\infty} \rho_m^2(v) \\
& \cdot g_1^2(r, v, \theta, \varphi) v dv d\theta. \tag{D.3}
\end{aligned}$$

As shown in Figure 2,  $v = 2r \cos(\theta - \varphi)$  for  $l_i = r$ . Thus, the limits of  $v$  are from  $\max[d, |2r \cos(\theta - \varphi)|]$  to  $\infty$ , since the closest interfering BS is at least at distance  $r$ . So the coverage probability can be approximated as

$$P_1(\text{SINR}_d > T) \approx \int_0^{2\pi} \int_0^{\infty} \lambda_m r e^{-\pi \lambda_m r^2} \omega dr d\varphi. \tag{D.4}$$

## E. Proof of Proposition 5

$$\begin{aligned}
& \mathbb{E}_{\Phi_m}^{\text{lo}} \left( \prod_{i \in \Phi_m} \frac{1}{1 + Tr^\alpha l_i^{-\alpha}} \right) \\
& = \mathbb{E}_{\Phi_m}^{\text{lo}} \left[ \exp \left( - \sum_{i \in \Phi_m} \ln(1 + Tr^\alpha l_i^{-\alpha}) \right) \right] \\
& \stackrel{(a)}{\geq} \exp \left\{ \mathbb{E}_{\Phi_m}^{\text{lo}} \left[ - \sum_{i \in \Phi_m} \ln(1 + Tr^\alpha l_i^{-\alpha}) \right] \right\}, \tag{E.1}
\end{aligned}$$

where (a) follows Jensen's inequality. Similar to Appendix D, let  $\eta = \mathbb{E}_{\Phi_m}^{\text{lo}} [-\sum_{i \in \Phi_m} \ln(1 + Tr^\alpha l_i^{-\alpha})]$ ; according to (D.3) we can get

$$\begin{aligned}
\eta & = \lambda_m^{-1} \int_0^{2\pi} \int_{\max[d, |2r \cos(\theta - \varphi)]}^{\infty} \rho_m^2(v) g_1(r, v, \theta, \varphi) \\
& \cdot v dv d\theta. \tag{E.2}
\end{aligned}$$

## Data Availability

Our data are obtained through simulation experiments and are available from the corresponding author upon request.

## Conflicts of Interest

The authors declare that they have no conflicts of interest.

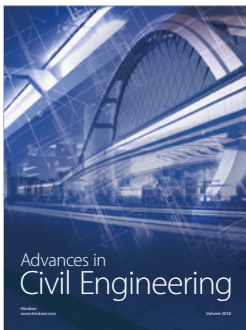
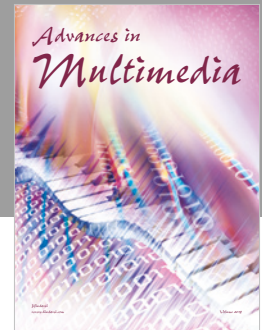
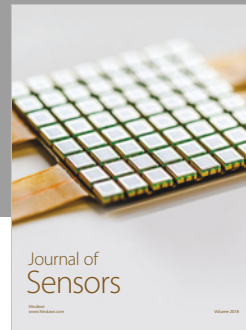
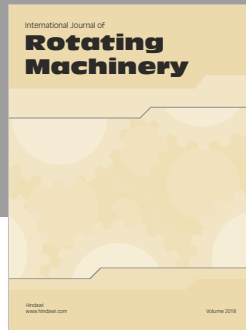
## Acknowledgments

This work has been supported by the National Natural Science Foundation of China under Grants nos. 61372092 and 61531013.

## References

- [1] Cisco, "Cisco visual networking index: Global mobile data traffic forecast update 2015-2020," white paper, 2016.
- [2] J. G. Andrews, S. Buzzi, and W. Choi, "What will 5G be?" *IEEE Journal on Selected Areas in Communications*, vol. 32, no. 6, pp. 1065-1082, 2014.
- [3] S. Woo, E. Jeong, S. Park, J. Lee, S. Ihm, and K. Park, "Comparison of caching strategies in modern cellular backhaul networks," in *Proceedings of the 11th Annual International Conference on Mobile Systems, Applications, and Services (MobiSys '13)*, pp. 319-332, Taipei, Taiwan, June 2013.
- [4] E. Bastug, M. Bennis, and M. Debbah, "Living on the edge: the role of proactive caching in 5G wireless networks," *IEEE Communications Magazine*, vol. 52, no. 8, pp. 82-89, 2014.
- [5] G. Paschos, E. Bastug, I. Land, G. Caire, and M. Debbah, "Wireless caching: Technical misconceptions and business barriers," *IEEE Communications Magazine*, vol. 54, no. 8, pp. 16-22, 2016.
- [6] K. Shanmugam, N. Golrezaei, A. G. Dimakis, A. F. Molisch, and G. Caire, "FemtoCaching: wireless content delivery through distributed caching helpers," *IEEE Transactions on Information Theory*, vol. 59, no. 12, pp. 8402-8413, 2013.
- [7] N. Golrezaei, A. G. Dimakis, and A. F. Molisch, "Scaling behavior for device-to-device communications with distributed caching," *IEEE Transactions on Information Theory*, vol. 60, no. 7, pp. 4286-4298, 2014.
- [8] N. Giatsoglou, K. Ntontin, E. Kartsakli, A. Antonopoulos, and C. Verikoukis, "D2D-Aware Device Caching in mmWave-Cellular Networks," *IEEE Journal on Selected Areas in Communications*, vol. 35, no. 9, pp. 2025-2037, 2017.
- [9] N. Golrezaei, P. Mansourifard, A. F. Molisch, and A. G. Dimakis, "Base-station assisted device-to-device communications for high-throughput wireless video networks," *IEEE Transactions on Wireless Communications*, vol. 13, no. 7, pp. 3665-3676, 2014.
- [10] J. Jiang, S. Zhang, B. Li, and B. Li, "Maximized cellular traffic offloading via device-to-device content sharing," *IEEE Journal*

- on *Selected Areas in Communications*, vol. 34, no. 1, pp. 82–91, 2016.
- [11] D. Malak and M. Al-Shalash, “Optimal caching for device-to-device content distribution in 5G networks,” in *Proceedings of the IEEE Globecom Workshops (GC Wkshps '14)*, pp. 863–868, Austin, Tex, USA, December 2014.
- [12] Z. Chen, N. Pappas, and M. Kountouris, “Probabilistic caching in wireless D2D networks: Cache hit optimal versus throughput optimal,” *IEEE Communications Letters*, vol. 21, no. 3, pp. 584–587, 2017.
- [13] Z. Yang, H. Tian, S. Fan, and G. Chen, “Distributed cooperative caching in backhaul-limited small cell networks,” *IEEE Electronics Letters*, vol. 53, no. 3, pp. 158–160, 2017.
- [14] J. G. Andrews, F. Baccelli, and R. K. Ganti, “A tractable approach to coverage and rate in cellular networks,” *IEEE Transactions on Communications*, vol. 59, no. 11, pp. 3122–3134, 2011.
- [15] E. Bastug, M. Bennis, and M. Debbah, “Cache-enabled small cell networks: Modeling and tradeoffs,” in *Proceedings of the 2014 11th International Symposium on Wireless Communications Systems, ISWCS 2014*, pp. 649–653, Barcelona, Spain, August 2014.
- [16] D. Malak, M. Al-Shalash, and J. G. Andrews, “Optimizing content caching to maximize the density of successful receptions in device-to-device networking,” *IEEE Transactions on Communications*, vol. 64, no. 10, pp. 4365–4380, 2016.
- [17] K. Li, C. Yang, Z. Chen, and M. Tao, “Optimization and analysis of probabilistic caching in N-Tier heterogeneous networks,” *IEEE Transactions on Wireless Communications*, vol. 17, no. 2, pp. 1283–1297, 2018.
- [18] H. ElSawy, A. Sultan-Salem, M.-S. Alouini, and M. Z. Win, “Modeling and analysis of cellular networks using stochastic geometry: a tutorial,” *IEEE Communications Surveys & Tutorials*, vol. 19, no. 1, pp. 167–203, 2017.
- [19] M. Haenggi, “Mean interference in hard-core wireless networks,” *IEEE Communications Letters*, vol. 15, no. 8, pp. 792–794, 2011.
- [20] B. Cho, K. Koufos, and R. Jantti, “Bounding the mean interference in Matern Type II Hard-Core Wireless Networks,” *IEEE Wireless Communications Letters*, vol. 2, no. 5, pp. 563–566, 2013.
- [21] M. Chen, Y. Hu, and C. Yin, “Tri-sectoring and power allocation of macro base stations in heterogeneous cellular networks with matern hard-core processes,” in *Proceedings of the 83rd IEEE Vehicular Technology Conference, VTC Spring 2016*, Nanjing, China, May 2016.
- [22] L. Breslau, P. Cao, L. Fan, G. Phillips, and S. Shenker, “Web caching and Zipf-like distributions: evidence and implications,” in *Proceedings of the 18th Annual Joint Conference of the IEEE Computer and Communications Societies (INFOCOM '99)*, vol. 1, pp. 126–134, New York, NY, USA, March 1999.
- [23] S. Singh, H. S. Dhillon, and J. G. Andrews, “Offloading in heterogeneous networks: modeling, analysis, and design insights,” *IEEE Transactions on Wireless Communications*, vol. 12, no. 5, pp. 2484–2497, 2013.
- [24] J.-S. Ferenc and Z. Néda, “On the size distribution of Poisson Voronoi cells,” *Physica A: Statistical Mechanics and its Applications*, vol. 385, no. 2, pp. 518–526, 2007.
- [25] I. S. Gradshteyn and I. M. Ryzhik, *Table of Integrals, Series, and Products*, Academic Press, 7th edition, 2007.
- [26] A. M. Ibrahim, T. ElBatt, and A. El-Keyi, “Coverage probability analysis for wireless networks using repulsive point processes,” in *Proceedings of the 2013 IEEE 24th Annual International Symposium on Personal, Indoor, and Mobile Radio Communications, PIMRC 2013*, pp. 1002–1007, London, UK, September 2013.
- [27] D. Malak, M. Al-Shalash, and J. G. Andrews, “Spatially Correlated Content Caching for Device-to-Device Communications,” *IEEE Transactions on Wireless Communications*, vol. 17, no. 1, pp. 56–70, 2018.



**Hindawi**

Submit your manuscripts at  
[www.hindawi.com](http://www.hindawi.com)

